Scrape-Off Layer Properties of Single-Null and Snowflake Diverted Plasmas in TCV

B. Labit, I. Furno, H. Reimerdes, W. Vijvers, S. Coda and the TCV team

École Polytechnique Fédérale de Lausanne (EPFL), Centre de Recherches en Physique des Plasmas (CRPP), Association EURATOM-Confédération Suisse, CH-1015 Lausanne, Switzerland.

Introduction The snowflake (SF) divertor [1, 2] is an innovative solution to reduce plasma-wall interaction by acting on the magnetic field topology to improve the divertor action. In this configuration, both the poloidal magnetic field and its spatial first derivatives vanish at the null point. The separatrix divides the poloidal plane in six regions and, as a consequence, the configuration has four divertor legs. Compared to a Single-Null (SN) configuration, the snowflake configuration is characterized by a larger flux expansion around the null point, a longer connection length in the scrape-off layer (SOL) and a larger magnetic shear close to the separatrix. These properties are expected to affect the local heat load on the divertor plates, in particular during Edge Localized Modes (ELMs). In the first part, we estimate, from Langmuir probe (LP) measurements, the heat loads during ELMy H-mode SN and SF plasmas. In the second part, we report on statistical properties of SOL fluctuations measured with LP and a fast imaging camera.

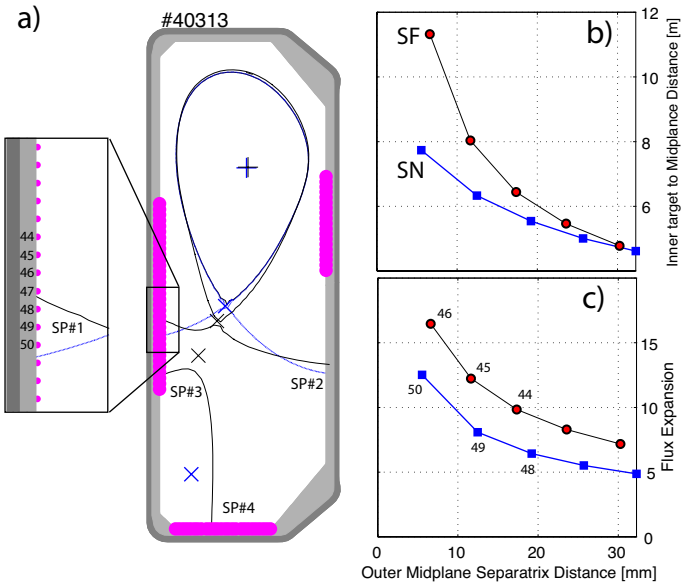

Figure 1: *a) Plasma separatrix for SN and SF plasmas together with location of Langmuir probes; b) Distance along the field lines from the inner target to the outboard midplane for SN and SF plasmas; c) Flux expansion.*

Inner target heat load estimate in ELMy H-mode plasmas It has been demonstrated in TCV that SN and SF configurations have a similar H-mode power threshold, whereas the SF confinement is 15% higher [3] . The most striking difference is in the ELM frequency, reduced by a factor 2-3 with the snowflake divertor, while the ratio of the energy lost per ELM to the plasma energy is only increased by 20-30%. As illustrated in Fig.1a), the HFS probes (34 probes, 4 mm tip diameter, vertically separated by 17.3 mm) provide a good coverage of the inner divertor target zones for the SN/SF diverted configurations. The distance from the outboard midplane to the inner strike point and the flux expansion for both configurations are shown in Fig.1b-c). For ELMy SN/SF plasmas, LP measurements at the inner target zone are

performed on a shot-to-shot basis. Three quantities are measured: the ion saturation current density J_{sat}, the floating potential V_{fl} and the current density at zero bias J_0 . These quantites are coherently averaged over ELMs detected on the D_α signal. Results are summarized in Fig. 2a-d). From D_α, it is seen that the duration of the ELM cycle is shorter ($\sim$1 ms) for the SN configuration compared to the SF one ($\sim$4 ms), consistent with the change of ELM frequency between the two configurations. The J_{sat} peak at the ELM crash is reduced by a factor 2 in SF H-mode compared to the single-null divertor, consistent with particle flux redistribution to the aditionnal strike points. For the SN plasma, the e-folding characteristic length of the J_{sat} profile (not shown) does not change significantly between the pre-ELM phase and the ELM crash (about 4 mm). By contrast, in the SF plasma, this length is doubled during the ELM crash (from 5 mm to 10 mm). The profile of $V_{fl}$and J_0 is more difficult to interpret. Just before the ELM crash both quantities increases close to the strike point but decrease further outside for the two configurations. The temperature is estimated with $T_e = \frac{eV_{fl}}{\ln(1-J_0/J_{sat})}$ (Fig.2d)) and the denstiy with $n_e = J_{sat}/(ec_s)$ where $c_s = \sqrt{e(T_e+T_i)/m_i}$ is the ion sound speed (assuming $T_e = T_i$). Finally, the heat load is estimated with the formula: $P_\perp = \gamma J_{sat} T_e / e \sin\alpha$ where $\gamma \simeq 5$ is the sheath heat transmission factor [4] and $\alpha \simeq 3-5^\circ$ is the angle between the total magnetic field and the wall [5]. The temperature elevation at the ELM crash is a factor 2 smaller for the SF configuration compared to the SN one. Consequently, the density evolution is nearly the same for both configurations. The estimated heat power is reduced by a factor 10 in the SF case. It has to be noted that the T_e peak is delayed with respect to the J_{sat} peak for the snowflake divertor, whereas the two are simultaneous for the SN divertor. This might suggest a modification of the transport mechanism for particles and heat

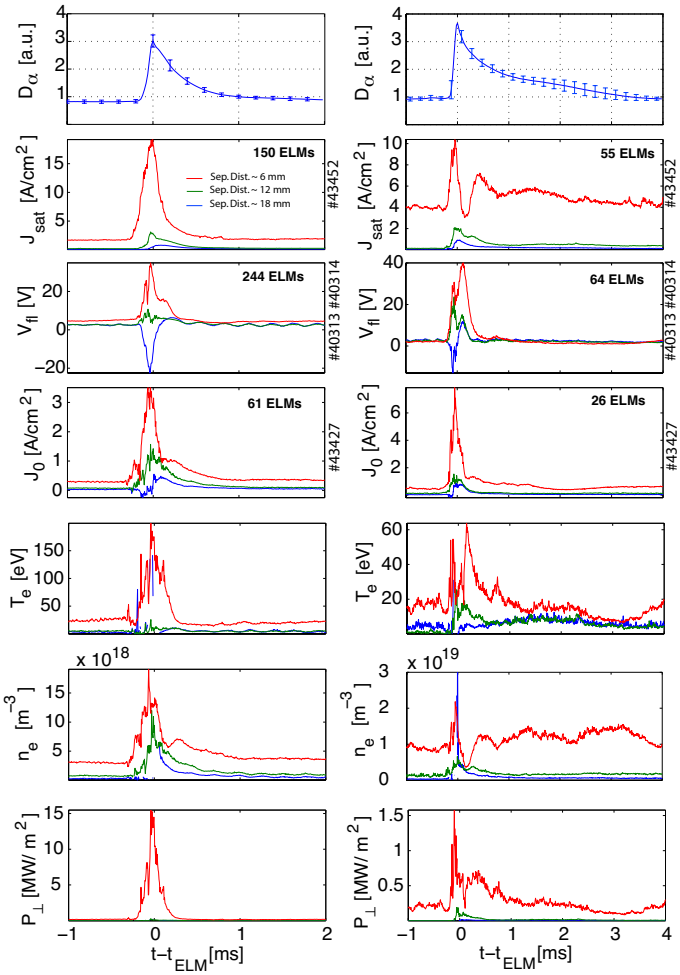

Figure 2: *ELM averaged measurements: a) D_α, b) J_{sat}, c) V_{fl}, d) J_0 for SN (left) and SF (right) plasmas. Derived quantities: e) T_e, f) n_e and g) $P_\perp$. Note the different x and y scales.*

during the snowflake diverted plasmas. This observation will be cross-checked with infrared measurements around strike points 1, 3 and 4 which are under analysis.

Midplane SOL statistical properties in ohmic L-mode plasmas In L-mode plasmas, the intermittent particle and heat SOL transport is associated with the presence of blobs propagating in the radial direction. We are comparing some statistical properties of J_{sat} fluctuations measured in SN and SF configurations with LP in the SOL at the LFS midplane. The radial distance between the last closed flux surface (LCFS) and the LP is about 2 cm (Fig.3 a)). Figure 3 b-c) displays J_{sat} measured on tip 62 for both plasma phases (SN and SF). The intermittent nature of transport is clearly visible with large J_{sat} spikes associated with density blobs propagating radially towards the wall. In order to investigate the influence of the plasma collisionality on the intermittent transport, a density scan is performed. The average and r.m.s. values of J_{sat} increase with density while the skewness, which is a measure of the intermittency, remains almost constant at a high level (not shown). Moreover, the level of fluctuations is significantly lower for the SF configuration compared to the SN one, which suggests that large amplitude blobs are less frequent two centimeters away from the LCFS in the SF configuration. Two reasons might be invoked to explain this observation: either blobs are convected faster to the strike points in the SF than in a SN configuration and therefore do not have time to reach the wall or, since the magnetic shear is larger for the SF plasma, blobs are more efficiently sheared-off and then dissipated. The conditional sampling technique is applied to J_{sat} signals from probes 61-64 for the lower and higher densities. Probe 62 is chosen as reference and the threshold for blob selection is set to 4σ, where σ is the standard deviation. The selected threshold results in about 250 blobs detected in a 300 ms long time trace. Results are summarized on Fig. 3d-g). The auto conditional sampling for signal from probe 62 gives an insight into the average blob's time

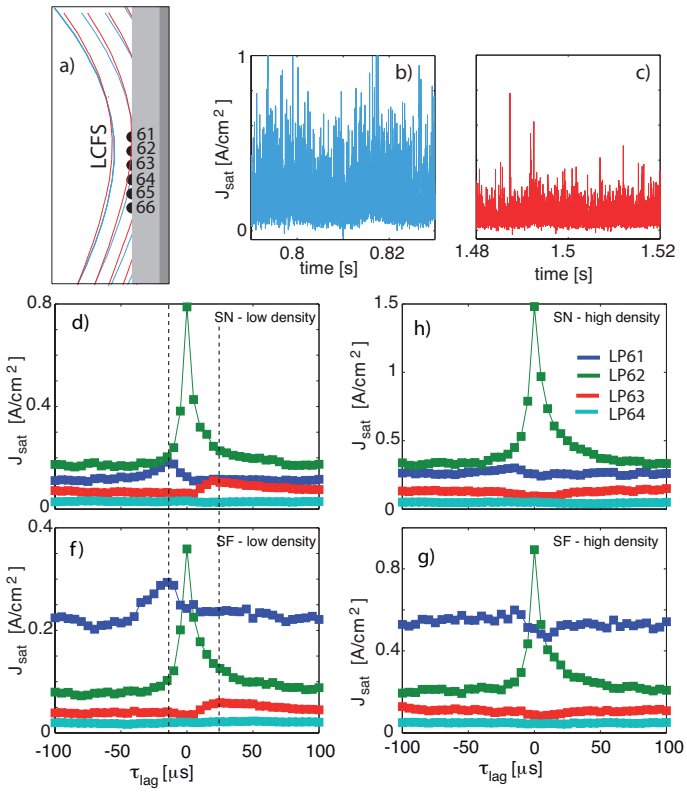

Figure 3: *(a) Detail of the location of the LP with respect to the LFCS; Example of J_{sat} measured during the SN phase (b) and the SF phase (c); Conditional sampling of J_{sat} for probes 61-64 for the low density (d, f) and for high density (e, g). The reference probe is 62.*

history. It is rather short ($\sim$30 μs) and its asymmetric evolution in time is more pronounced at high density and for the SF configuration. For both configurations and at low density, the blob is seen about 20 μs earlier on probe 61 and about 20 μs later on probe 63 with respect to the reference probe as indicated by the vertical dashed lines in Fig. 3 d-e). This corresponds to a propagation velocity of about 800 m/s. This observation indicates that blobs propagate not only in the radial direction but also in both toroidal and poloidal directions. At higher density, no more correlation is observed between probes suggesting a higher level of blob dissipation along the magnetic field lines.

To complete the analysis of SN/SF L-mode plasmas, we briefly report on measurements with a fast framing camera (Photron APX-RS). The camera looks tangentially at the plasma with a wide angle of view (Fig4a)). All visible light is collected without any filtering. The framing rate is set to 30kf/s implying a reduction of the chip to 86x140 pixels (white rectangle in Fig.4a)). The normalized level of light fluctuation is slightly higher in the SN phase compared to the SF one and seems to be localized at the plasma edge (insets in Fig.4a)). Tomographic inversion is under consideration for a clearer interpretation. In Fig.4b), the skewness is represented. It clearly changes from negative values to positive values as the separatrix is crossed, similarly to what has been observed with LP measurements in other tokamaks. Finally, the frequency spectrum of the measured light in the region of almost zero skewness reveals some coherent fluctuations around 6 kHz. It has to be noted that this mode is also detected on magnetic probes.

This work is partly funded by the Fonds National Suisse de la Recherche Scientifique

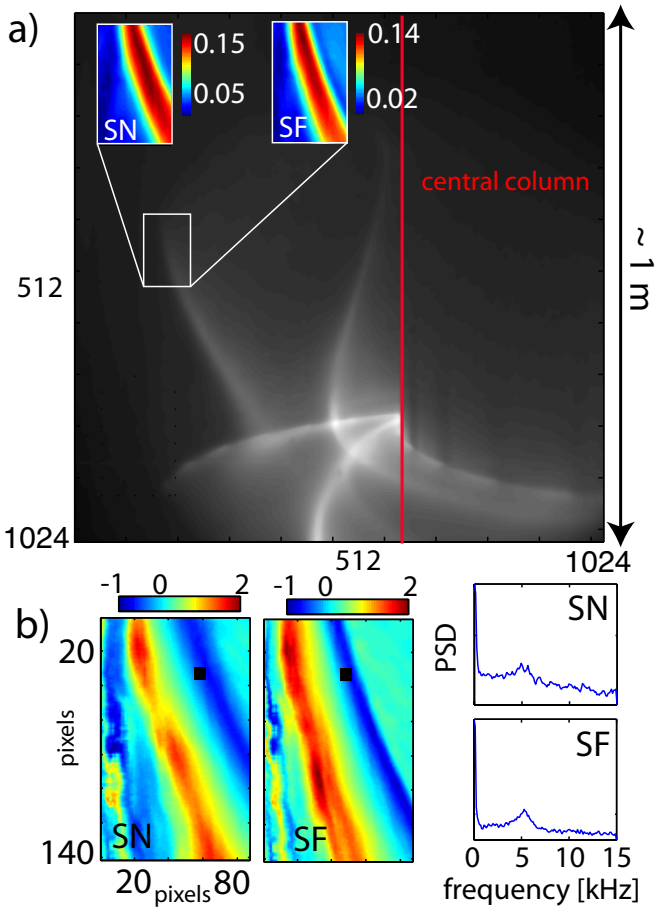

Figure 4: *a) Fast camera image (1024×1024 3kfps); Inset) Light rms normalized to the average light; b) Skewness and frequency spectrum of measurement in the black square shown in c).*

References

[1] Ryutov D. D. *et al.*, Phys. Plasmas **15**, 092501 (2008)
[2] Piras F. *et al.*, Plasma Phys. Control. Fusion **51**, 055009 (2009)
[3] Piras F. *et al.*, Phys. Rev. Lett. **105**, 155003 (2010)
[4] Marki J. *et al.*, Journal of Nucl. Mat. **363**, (2007) 382
[5] Pitts R. A. *et al.*, Nucl. Fusion **43**,1145 (2003)